

# Potential Application of Rice Husk for Synthesis of Catalyst for Biodiesel Production

Jibril Goli Buta, Nedumaran Balasubramanian

**Abstract** -- This study synthesizes biodiesel from soybean oil using transesterification over rice husk based  $\text{Li}_2\text{SiO}_3$  and  $\text{Na}_2\text{SiO}_3$  catalysts. The catalysts were characterized using FTIR, powder-XRD, DTA/TGA, XRF and SEM instruments. At optimum condition of 500°C catalyst calcination, 3wt% catalyst concentration, 60°C reaction temperature, 150min reaction time and 12:1 methanol to oil molar ratio; the biodiesel yield of 96.7% was obtained for rice husk derived sodium silicate catalyst, whereas for rice husk derived lithium silicate catalyst, the biodiesel yield of 99.4% was obtained at optimum condition of 4wt% catalyst concentration, reaction temperature of 65°C, reaction time of 180min and methanol to oil ratio of 24:1. The biodiesel products were also characterized by using H-NMR, FTIR and GC-MS and the results confirm the transformation of oil triglyceride to biodiesel methyl ester. The physicochemical properties of biodiesel fuels were also in agreement with international standard.

**Index Terms** -- Agricultural waste, rice husk ash, catalyst, sodium silicate, lithium silicate, soybean oil, transesterification, biodiesel fuel

U

## 1. INTRODUCTION

Now a days, biodiesel is considered as a renewable biofuel with fewer pollutant emission than petrol diesel.

The use of *rice husk* (RH) from agricultural waste as a catalytic material is one way to reduce the cost of the catalyst and keep the environment clean. This approach creates additional revenue opportunities for farmers, entrepreneur and local government in addition to reducing the cost of procuring and synthesizing the catalytic material. Instead of discharging them, using waste material as a catalyst also lessens the cost of waste management.

The primary staple food for billions of people is rice and it covers 1% of the earth's surface [1]. Based on weight, RH account for nearly 20% of paddy production and it is the outer cover of the rice [2]. The heating value of 16.3MJ/kg, volatile matter content of 74% and ash content of 20% are the main characteristics of the RH [3]. It is used as a fuel to produce steam in various industries and this characteristics indicate that the RH could be a good solid fuel [4], and therefore, conserving both energy and resources. Rice husk ash, which is typically considered as waste, produced when RH is burnt in air [5]. It is the only crop by product that generates a huge quantity of ash when it is burnt in air [6]. Silica (87-99%) and minor amount of inorganic salts are the main constituents of RH ash [7], [8]. Suitable substitute disposition must be scheduled to avoid undesirable environmental effect as about 70 million tons of RH ash is being produced annually.

Nedumaran Balasubramanian, School of Mechanical Chemical and Materials Engineering, Adama Science and Technology University, Adama, Ethiopia. E-mail: nedumaran\_b@yahoo.co.in (Corresponding Author)

Inorganic metal such as  $\text{Pd}^{2+}$  and  $\text{Cu}^{2+}$  metal ions [9], [10], absorbent to absorb organic dye such as malachite green [11], as construction material in concrete [1], [12] are the application area where the RH ash has been used so far. Silica from RH ash can be an additive for rice plant itself, as it is absorbed by the roots of plant and deposited on the outer walls of epidermal cells as a silica gel and act as a physical barrier against pathogenic fungi and attacks by insects [13]. In recent years, RH ash is used as economically viable raw material for producing silicates and pure reactive silica [14] because of its high silica content [15]. Sodium silicate is a very popular water glass which can be prepared in a simple manner from  $\text{SiO}_2$  and  $\text{NaOH}$  [16]. In order to synthesize mesoporous silica material [17],  $\beta$ -zeolite [18], normal alkane-silica composite phase [19]; sodium silicate was also used as reactant. In the transesterification reaction of vegetable oil, the use of calcined sodium silicate as solid basic catalyst has been reported recently, implies that the effectiveness of the catalyst under mild reaction condition and short reaction time, the reusability of the catalyst without the loss of its activities was for at least about 5 times [20], [21], [22].

The key objective of this study is to develop heterogeneous catalyst from RH. Two types of heterogeneous alkali catalyst are prepared from RH ash based chemical reaction; lithium silicate catalyst is prepared using lithium carbonate as an activating agent and sodium silicate is prepared using sodium hydroxide as an activating agent through a solid state reaction.

Jibril Goli Buta, Chemical Engineering Program, School of Mechanical Chemical and Materials Engineering, Adama Science and Technology University, Adama, Ethiopia. E-mail: jibrilgoli430@gmail.com

## 2. MATERIALS AND METHODS

### 2.1. Materials

Soybean oil was purchased from local market in Roorkee city, India. The density and molecular weight of the oil were measured to be 0.902g/ml and 871.99g/mole respectively. RH from local rice mill, utilized as catalyst source. Methanol, NaOH, Li<sub>2</sub>CO<sub>3</sub> and HCl (all analytical reagent) were purchased from local market in Roorkee, Uttarakhand State, India (Thomas baker chemical, Bharat Mahal, Marine Drive, Mumbai, India).

### 2.2. Preparation and Characterization of RH derived catalyst

Na<sub>2</sub>SiO<sub>3</sub> catalyst preparation method (RH-Na<sub>2</sub>SiO<sub>3</sub>)

Clay particles and residuals rice were eliminated by sieving the RH using sieve screen. Then the residual, clay free RH was washed with deionized water and allowed to dry overnight for 12h at 110°C in oven. The oven dried RH was digested by reflux technique in 1M HCl (solution prepared from 83.5ml of 35.4% concentrated HCl and distilled water in 1L borosilicate glass). The digested RH was washed with deionized water several times until the pH of washing water becomes neutral and acid free RH was again dried in hot oven at 110°C overnight for 12h. The digested-oven dried RH was converted to RH ash after calcining at 700°C for 4h; where organic matter were removed during heat treatment [23]. To generate the sodium silicate material, 7g of prepared RH ash and 90ml of 1M NaOH were mixed and boiled for 1h with constant stirring in 500ml borosilicate flask. Then drying of the subsequent solution was carried out in an oven for 6h at 110°C. To obtain the heterogeneous alkali catalytic material, the resulting material was calcined in a furnace within temperature range of 400-550°C in air for 1h.

Li<sub>2</sub>SiO<sub>3</sub> catalyst preparation method (RH-Li<sub>2</sub>SiO<sub>3</sub>)

This follows the same procedures as for sodium silicate preparation up to the hot oven drying of acid free acid RH at 110°C for 2h. Then a sample of RH was converted to RH ash by calcining RH at 900°C for 4h. Again the resulting material was washed with deionized water and filtered and the RH ash was dried at 120°C for 16h in oven. In order to obtain highly active solid lithium silicate catalyst, 1.0g of RH ash was well mixed and ground with 1.23g of Li<sub>2</sub>CO<sub>3</sub> using ceramic pastel mortar. The resulting slurry was then calcined at 900°C in air atmosphere for 4h.

### 2.3. Catalysts Characterization

The developed catalysts were characterized through X-ray fluorescence (XRF) spectroscopy, thermal gravimetric analysis

(TGA)/ differential thermal analysis (DTA), Fourier Transform infrared spectroscopy (FTIR), Scanning electron microscopy (SEM) and X-ray diffraction (XRD). The XRF analysis was performed by using a BRUKER S4 PIONEER spectrometer to identify the major and minor elements present as oxide form in sample under investigation. X-ray fluorescence was performed under energy dispersive mode for accurate measurement of minor and major element present in the sample. The TGA/DTA was performed on differential thermal analyzer of type (SII 6300 EXSTAR) to estimate the complete decomposition temperature of RH, mixture of RH ash-NaOH and mixture of RH ash-Li<sub>2</sub>CO<sub>3</sub> through temperature program of 25 – 700°C for pure RH and mixture of RHA-NaOH, whereas 25-900°C for mixture of RHA-Li<sub>2</sub>CO<sub>3</sub> with 10°C/min of constant heating rate and under nitrogen flow as inert gas. XRD analysis was performed on Bruker D8 Advance which was powder diffractometer. A source of Cu-K $\alpha$  radiation was used. The scan was taken from 2 $\theta$  = 5 to 2 $\theta$ = 90 with step size of 0.019°, step time of 38.4s and at room temperature of 25°C. Powder X-ray diffraction equipment was used for the identification of phase present in the catalyst. The FTIR equipment (THERMO SCIENTIFIC-NICOLET 6700) was used within the wave number range of 500 to 4000 cm<sup>-1</sup> for the determination of functional group and investigation of major absorption band for RH and its derived catalyst. SEM analysis was performed on SEM equipment (LEO 435VP). The topographical information (a high resolution image of the surface of a catalyst), information about catalytic particle morphology, composition near the surface region of the material and the active phase homogeneity were studied by using SEM (Scanning Electron Microscope).

### 2.4. Transesterification of Oil to Biodiesel

Three necked glass reactor equipped with condenser, thermometer and magnetic stirrer was used for the transesterification of soybean oil to biodiesel. For both catalyst, the reactor was primarily filled with 13g of soybean oil and on which the mixture of methanol and catalyst were added to the preheated oil. To avoid the splashing in the flask at the stirring speed, the reactant was stirred evenly. As soon as the mixture of methanol and the catalyst were added to the reactor, the timing of the reactor was initiated. The effect of reaction temperature (45 to 75°C), MeOH to oil ratio (6:1 to 30:1), catalyst concentration (1-5wt %), reaction time of (30-300min) on the conversion of triglyceride to biodiesel were studied. All of the experiments were investigated at atmospheric pressure. The yield of biodiesel is calculated by [24].

$$\text{Biodiesel yield} = \frac{\text{weight of biodiesel produced}}{\text{weight of oil used}} \times 100 \quad (1)$$

### 3. RESULT AND DISCUSSION

#### 3.1. Characterization of Catalysts

When calcined up to 700°C, the RH loss its mass up to 83.16% by weight (Fig.1). Loss of physically absorbed moisture and water content in the RH was up to 200°C. Of the total weight loss, this loss was account 5.63% by weight. The removal of organic group by oxidation reaction and removal of water formed from poly condensation reaction was corresponds to weight loss from 200 to 600°C. In between from 200 to 300°C, the decomposition of hemicellulose takes place. From 300 to 351°C, the decomposition of cellulose and decomposition of most of the volatile material takes place. From 351 to 600°C, the TG curve represent the volatilization of cellulose and followed by total decomposition of lignin. Above this temperature range, the remaining residue was considered as a char [2], [25], [26], [27], [28]. Finally, from TGA curve it has shown that, beyond 600°C, the RH loss no more weight. Therefore, calcining RH at approximately 700°C gives a RH ash which contain high composition of SiO<sub>2</sub> in side it [23]. From DTG curve, the rate of weight loss was maximum at 337°C and was amount to 177.3µg/cel. As per the result of DTA curve, there were two exothermic peak; initially at 373°C due to transformation of organic matter to volatile organic substance and next at 528°C due to carbonization [29].

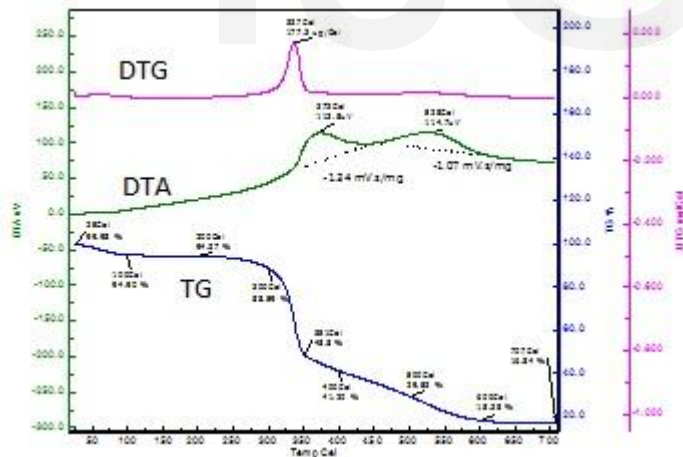


Fig. 1. DTG/DTG/TG curve for acid digested rice husk

After boiled for 1h at 100°C, and hot oven dried at 110°C for 6h, the mixture of RH ash and sodium hydroxide powder was analyzed by TGA/DTA to determine the thermal behavior of the resulting material (Fig. 2). There was only one weight loss at below 500°C which was due to loss of water molecules and physically absorbed moisture from the resulting material. This loss was equivalent to 9.18% by weight. Beyond 500°C, the weight loss of the resulting mixture was almost constant;

which gives the direction for the formation of sodium silicate when calcined just above this temperature. From DTG curve, the rate of weight loss was maximum at 337°C and was about 4.84µg/cel. Therefore, based on these graph result, to optimize the calcining temperature for the generation of sodium silicate, the temperature of 400, 450, 500 and 550°C were selected [22].

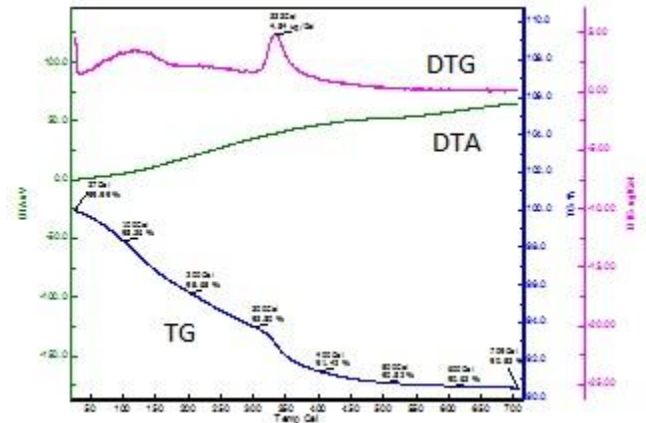


Fig. 2. DTG/DTG/TG curve for mixture of rice husk ash and sodium hydroxide.

The thermal behavior of mixture of calcined RH ash and lithium carbonate was shown in Fig. 3. The purpose is to estimate the calcination temperature used to generate lithium silicate from this mixture. As shown from TG curve, the first weight loss from 29°C to 600°C was about 3.16% by mass and it was attributed to dehydration process of water absorbed on the surface of lithium carbonate. Second weight loss observed between 600 to 765°C was attributed to decarbonization process which was present in lithium carbonate and was about 36.14% by weight. Above 800°C, the sample is thermally stable and no more weight loss has seen. Therefore, the thermally stable material was lithium silicate which was heterogeneous alkali catalyst used for biodiesel synthesis. Thus, for testing of catalytic activities, the chosen calcination temperature was 900°C. From DTG curve, the rate of weight loss was maximum at 716°C and was amounts to 105.2 µg/cel. Also from differential thermal analysis, thermal decomposition is endothermic reaction with heat absorption of 1.29 m.V.S/mg at 718°C. Because energy is required to release CO<sub>2</sub>, contained in lithium carbonate during the reaction with SiO<sub>2</sub> to form Li<sub>2</sub>SiO<sub>3</sub>.

As shown in Fig.4., all the material under consideration; RH ash, mixture of RH ash with sodium hydroxide calcined at 400, 450, 500 and 550°C shows different diffraction pattern. XRD pattern of RH ash and RH ash mixed with sodium hydroxide calcined at 400°C for 1h shows almost similar and at this condition no very sharp crystalline peak has observed. Therefore, no sodium silicate was detected when sample was calcined at 400°C ;thus, not enough to use this as a catalyst for

biodiesel synthesis. But clear, more crystalline and sharp peak were observed as the sample mixture were calcined at 450, 500 and 550°C. This indicate that after calcination, the mixture of RH ash and sodium hydroxide was changed to sodium silicate as their XRD pattern detect the diffraction pattern of sodium silicate.

for a catalyst due to its crystalline morphology. The position of 2theta value at which lithium carbonate with high intensity was identified were,  $2\theta = 21.5337, 29.6227, 30.7575, 31.9350, 34.3010, 36.2319$  and  $37.0921$  with reference code of 01-083-1454 JCXRDS. Fig. 5b., indicate the XRD pattern for mixture of RH ash and lithium carbonate with ratio of 1:1.23.

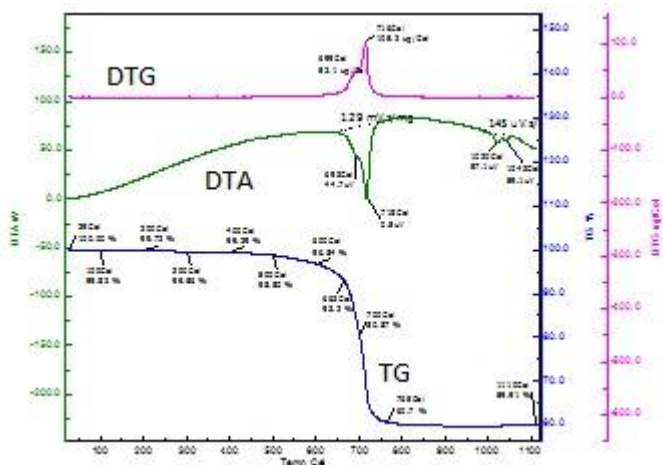


Fig. 3. DTA/DTG/TG curve for mixture of rice husk ash-Li<sub>2</sub>CO<sub>3</sub> (1:1.23)

After calcination at 700°C for 4h, 5g of RH ash was taken to XRF instrument to identify the major mineralogical component present in the sample. RH ash contain high concentration of SiO<sub>2</sub> which contributes about 91.09% by weight and other minor mineral oxides (Table 1). Therefore, from this result, it was evident that the RH ash was rich in silicon dioxide and thus this silicon dioxide can be reacted with sodium hydroxide and lithium carbonate by solid state reaction to generate sodium silicate and lithium silicate which are highly active heterogeneous alkali catalysts used in the transesterification reaction of vegetable oil; preferably, soybean oil in this study.

The presence of sodium silicate was detected at approximately diffraction angle of  $2\theta = 7.32, 20.0, 28.5, 39.45, 40.0, 50.0, 60.0,$  and  $69.7$  for the mixture calcined at 450, 500 and 550°C. But the calcination temperature of 500°C was chosen as the optimum temperature for the generation of highly crystalline sodium silicate catalyst, because at lower temperature of 450°C, there may not be the total removal of water from sodium silicate and at higher temperature of 550°C, the catalyst may get sintered hence this may lower the surface area.

The XRD pattern for lithium carbonate, mixture of lithium carbonate and SiO<sub>2</sub> from RH ash at a ratio of 1.23:1 and lithium silicate catalyst generated from calcination of RH ash (SiO<sub>2</sub>) and lithium carbonate at 900°C for 4h were shown in Fig.5. The result indicates that, from figure Fig.5a, the presence of lithium carbonate at all the  $2\theta$  values. The indication of clear and sharp peak suggest the lithium carbonate as a precursor

TABLE 1.

Serial No.	Chemical Component	Proportion, %
1	Silicon oxide	91.09
2	Sodium oxide	1.53
3	Potassium oxide	0.68
4	Iron oxide	1.32
5	Strontium oxide	0.31
6	Calcium oxide	0.36
7	Magnesium oxide	0.34
8	Aluminum oxide	0.36
9	Manganese oxide	0.61
10	Loss on ignition	3.4

CHEMICAL COMPOSITION OF RICE HUSK ASH

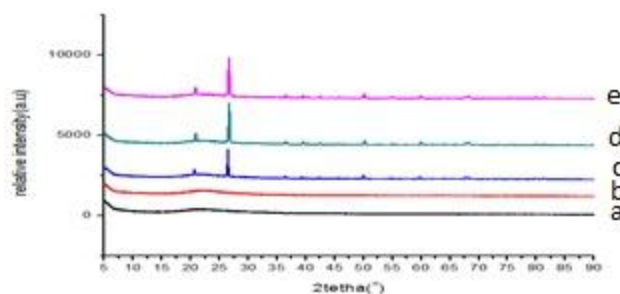


Fig. 4. XRD pattern ( $2\theta$ , degree Vs Relative Intensity, AU) of RHA (a), mixture calcined at 400°C (b), mixture calcined at 450°C (c), mixture calcined at 500°C (d), mixture calcined at 550°C (e).



calined at 500°C (d), mixture calcined at 500°C (e) for 1h (from bottom to top)

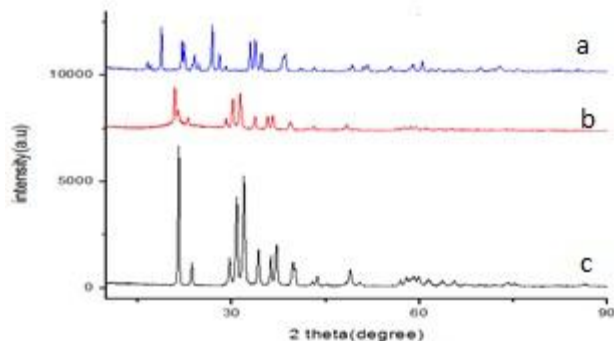


Fig. 5. XRD pattern (2Theta, degree Vs Intensity, AU) of  $\text{Li}_2\text{CO}_3$  (a), mixture of  $\text{Li}_2\text{CO}_3$  & RHA with ratio of 1:1.23(b), mixture of  $\text{Li}_2\text{CO}_3$  & RHA (with ratio of 1:1.23) calcined at 900°C for 4h (c) (from bottom to top)

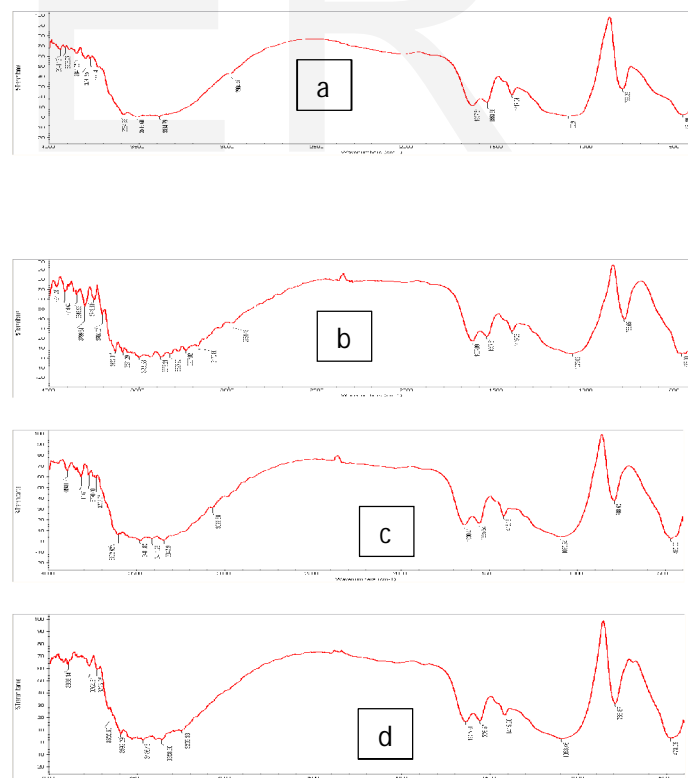
Also from Fig. 5c., it was seen that the presence of sharp, clear and highly crystalline peak. This diffraction pattern represents two form of lithium silicate compound ( $\text{Li}_2\text{SiO}_3$  and  $\text{Li}_4\text{SiO}_4$ ); the products which were obtained after the calcination of RH ash and lithium carbonate at 900°C for 4h. Among them,  $\text{Li}_2\text{SiO}_3$  is the required chemical compound used as a catalyst for biodiesel synthesis. According to the Joint committee of XRD pattern of reference code 01-083-1517, the angle at which  $\text{Li}_2\text{SiO}_3$  catalyst detected were;  $2\theta = 18.7702, 26.8867, 32.9398$  and  $38.5700$ . The relative intensity for this  $2\theta$  value were just above 35%. Whereas for  $\text{Li}_4\text{SiO}_4$ , it was detected at an angle of  $2\theta = 22.0823, 22.4495, 24.0698, 28.0326, 33.7274$  and  $34.7479$  with reference code of 00-004-0727. The contribution of their relative intensity were above 36%.

The FTIR spectra of RH ash was shown in Fig. 6a. The presence of Si-H functional group was indicated at the bands of  $799.28$  and  $461.80\text{ cm}^{-1}$  [30]. The band at  $1102.91\text{ cm}^{-1}$  suggest that the presence of Si-O-Si functional group. The same result was obtained by [31]. The band at  $1417.04\text{ cm}^{-1}$  suggests the presence of stretching of aromatic ring [32]. Stretching of aldehyde and ketone is observed at  $1637.09$  and  $1557.31\text{ cm}^{-1}$ . The band at  $2984.46\text{ cm}^{-1}$  represent the presence of methyl group. Methyl group is present in the RH ash due to the presence of lignin [31]. The region of band spectra from  $3384.79$  to  $3584.96\text{ cm}^{-1}$  represent the presence of OH stretching due to silanol group (i.e., SiOH) and adsorption of water on the surface.

The spectra of all calcined sample to generate sodium silicate material which was used as a heterogeneous alkali catalyst for the transesterification reaction of soybean oil has shown in the Fig. 6 of (b),(c), (d), and (e). Stretching vibration of Si-O bond and Si-O-Si bond were observed at strong broad absorption band at  $1079.02$  and  $788.65\text{ cm}^{-1}$  respectively for sample calcined at 400°C, at  $1095.94$  and  $788.65\text{ cm}^{-1}$

respectively for sample calcined at 450°C, at  $1093.46$  and  $788.87\text{ cm}^{-1}$  respectively for sample calcined at 500°C and finally at  $1115.92$  and  $792.12\text{ cm}^{-1}$  for the sample calcined at 550°C. The band at  $1415.58, 1415.16, 1415.20$  and  $1468.52\text{ cm}^{-1}$  were assigned respectively to Si=O stretching vibration when sample were calcined at 400, 450, 500 and 550°C. The presence of Si-O-Si linking structure was indicated by these stretching vibration, thus the formation of sodium silicate was confirmed from this evidence [20]. for all sample calcined at different temperature, the broad peak from around  $3200$  to  $3600\text{ cm}^{-1}$  were attributed to Si-O-H stretching vibration caused due to the absorbed water molecules by the surface. There was reduction in the intensity of water peak in the region from sample calcined at 400°C to sample calcined at 550°C, this was due to dehydration of water molecules from the catalyst surface by calcination process.

The FTIR spectra for lithium silicate catalyst was displayed in graph of Fig.6c. The medium band at  $3443.45\text{ cm}^{-1}$  represent O-H vibration [32]. The asymmetric stretching mode of Si-O-Si functional group was observed at a peak of  $1063.76\text{ cm}^{-1}$  [33]. The presence of lithium silicate vibration was confirmed at the bands of  $1480.15$  and  $1439.69\text{ cm}^{-1}$  [34]. The presence of Si-O-Si bond and O-Si-O stretching vibration were confirmed at the bands of  $526.34, 615.59$  and  $735.28\text{ cm}^{-1}$ [34].



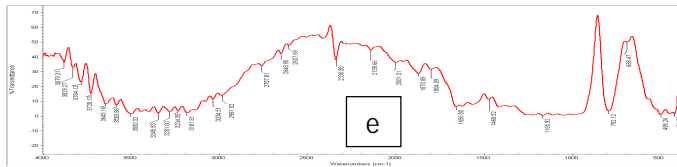


Fig. 6. FTIR spectra (Wavenumber,  $\text{cm}^{-1}$  Vs Transmittance, %) of rice husk ash (a), mixture calcined at  $400\text{ }^{\circ}\text{C}$  (b), mixture calcined at  $450\text{ }^{\circ}\text{C}$  (c), mixture calcined at  $500\text{ }^{\circ}\text{C}$  (d) and mixture calcined at  $550\text{ }^{\circ}\text{C}$  (e)

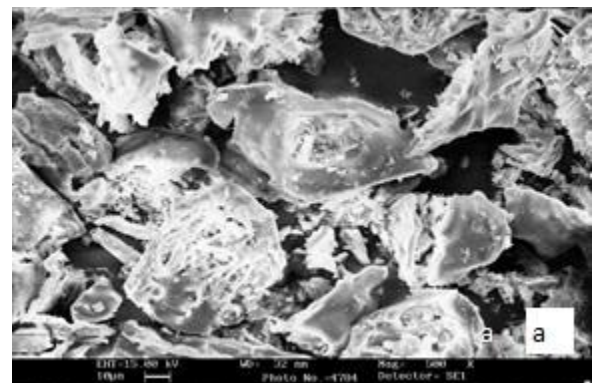
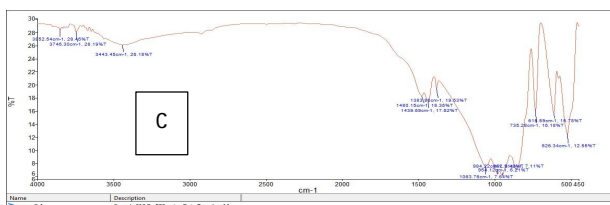
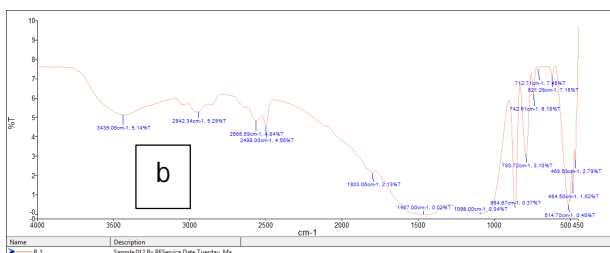
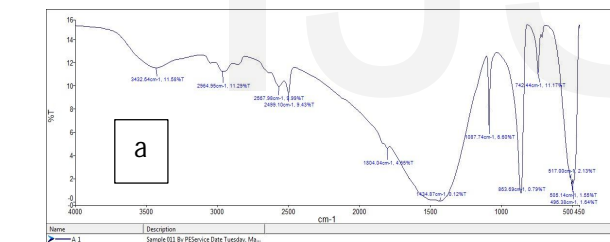
The morphological features of all powders; namely, RH ash, mixture of RH ash and sodium hydroxide after drying and finally the catalyst product (Sodium Silicate) obtained when mixture was calcined at  $500\text{ }^{\circ}\text{C}$  for 1h were shown in Fig 8. For RH ash, the SEM micrograph indicates that the presence of large spherical and impermeable porous surface. It has the layer thickness of 32nm and shows that the size of the sphere are nearly homogeneous with about  $10\mu\text{m}$ . after the solution has boiled and dried, the particle size was reduced to  $1\mu\text{m}$ . thread like and agglomerate surface was seen from SEM image. Finally the calcination at  $450\text{ }^{\circ}\text{C}$  brings, the morphology of the catalyst to agglomerate shape and these agglomerate were loosely attached. These structure create a favorable condition for the access of triglyceride and methanol, such that the basic sites of internal surface can be exploited for transesterification reaction.

Fig. 7. FTIR spectra of lithium carbonate (a), mixture of rice husk ash-lithium carbonate (b) and lithium silicate generated by solid state reaction of (b) at  $900\text{ }^{\circ}\text{C}$  for 4h (c)

The morphological features of all powders; namely, RH ash, lithium carbonate, mixture of lithium carbonate and RH ash and finally the catalyst product (lithium silicate) obtained by solid state reaction of lithium carbonate and RH ash calcined at  $900\text{ }^{\circ}\text{C}$  for 4h were shown in Fig.9. For RH ash, the SEM micrograph indicates that the presence of large spherical and impermeable porous surface. It has the layer thickness of 32nm and shows that the size of the sphere are nearly homogeneous with about  $10\mu\text{m}$ . for lithium carbonate powder, the SEM morphology suggests that the presence of small, aggregate and thread like structure with average particle size of  $2\mu\text{m}$ . the mixture of lithium carbonate and RH ash describes the features of both samples with small, aggregate, porous and spherical like structure with interconnected network of silicon dioxide in the RH ash and lithium carbonate. The corresponding particle size was about  $2\mu\text{m}$ . finally, after calcination, the solid state reaction bring the catalyst with very highly crystalline morphology, agglomerate and rod-thread like structure with average particle size of  $2\mu\text{m}$ .

#### 4. EFFECT OF PROCESS PARAMETER ON BIODIESEL YIELD

For the transesterification reaction of soybean oil, the catalytic activities of RH based sodium silicate was varied with calcination temperature. The catalytic activity of RH based lithium silicate catalyst was not evaluated with different calcination temperature, because, the catalyst was already calcined only at  $900\text{ }^{\circ}\text{C}$ . As the catalyst was calcined at  $400\text{ }^{\circ}\text{C}$ , the biodiesel yield was only 52% (Fig.10a).



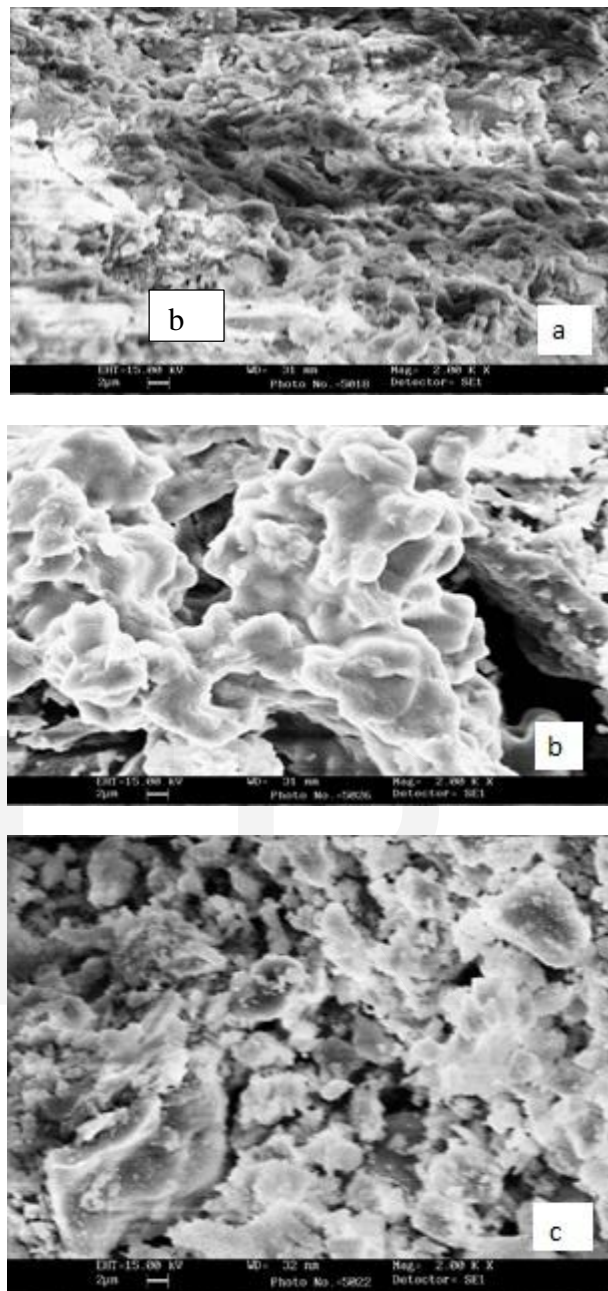
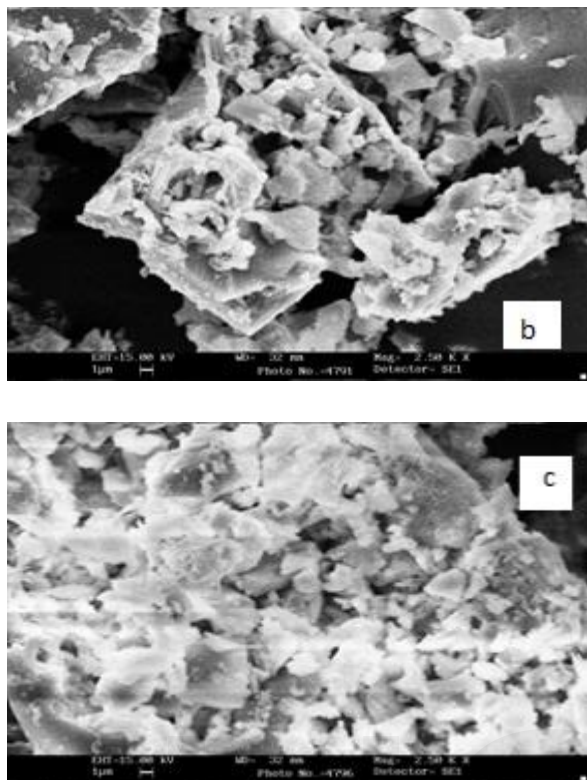


Fig. 8. SEM image (2500X) of rice husk ash (a), mixture of rice husk ash and sodium hydroxide after drying (b) and sodium silicate calcined at 500°C for 1h (c)

Since at this calcining temperature, there is low intensity peak in XRD pattern which indicates that low conversion of RH ash-sodium hydroxide mixture to sodium silicate catalyst. When calcining temperature of the sample increased from 400 to 500°C, significantly, the biodiesel yield was increased to 96.8%. This was because of the XRD pattern of the sample calcined at 450, 500 and 550°C indicate clear, sharp and highly crystalline and consequently confirm the conversion of sample to sodium silicate. Under the same reaction condition, further increase in calcination temperature result in slightly decrease in % biodiesel yield this was resulted from decreasing of catalyst surface area due to sintering effect at higher temperature. As a result, to synthesize the sodium silicate catalyst from the mixture of RH ash- sodium hydroxide, 500°C was taken as the optimal calcination temperature.

Fig. 9. SEM image of lithium carbonate (a), mixture of rice husk ash and lithium carbonate (b) and lithium silicate (c)

One of the utmost imperative parameter which affect both the reaction rate and yield is reaction temperature (Fig.10b). With constant reaction time of 45min and 3h respectively for sodium silicate and lithium silicate, the reaction temperature was varied from 45 to 75°C to investigate biodiesel yield. As the reaction temperature increased from 45 to 60°C for sodium silicate catalyst and 45 to 65°C for lithium silicate, the % biodiesel yield was increased from 40.5 to 96.7% and 50.7 to 99.3% respectively for sodium silicate catalyst and lithium silicate catalyst. Further increase the reaction temperature above 60°C and 65°C respectively for sodium silicate and



lithium silicate catalyst, give rise in the decreasing of biodiesel yield, because evaporated methanol inhibit the reaction on three phase interface; soybean oil-methanol-catalyst [35].

The effect of reaction time on the production of biodiesel from soybean oil using both RH based sodium silicate and lithium silicate catalyst were shown in fig.11b. After 150min, the biodiesel yield reach 96.3% for sodium silicate catalyst and the yield reach around 99.4% after 180 min for lithium silicate catalyst. For lithium silicate catalyst, the yield of biodiesel obtained was greater than 90.2% within 1h reaction time and as a result of equilibrium conversion, thereafter the reaction time became nearly the same. For sodium silicate catalyst, the yield of biodiesel was rapidly falls as the reaction time increase when compared to lithium silicate catalyst.

Methanol to oil molar ratio was one of the most important parameter affecting the yield of biodiesel in the transesterification reaction. As the molar ratio of methanol to soybean oil was increased from 6 to 24 for lithium silicate catalyst and from 6 to 12 for sodium silicate catalyst, the % biodiesel yield gradually increased (fig.11a). There was slight decreasing of the conversion of soybean oil if molar ratio was further increased beyond 12:1 for sodium silicate catalyst and beyond 24:1 for lithium silicate catalyst. This was due to dissolution of glycerol byproduct in excessive methanol and thus inhibition of the reaction of methanol with soybean oil and solid catalyst; if excessive methanol to oil ratio was used. Other reason for reduction of %biodiesel with excessive methanol to oil molar ratio is due to the presence of polar hydroxide in methanol which act as emulsifier which create difficulty in separating the biodiesel product from the reaction mixture; thus resulting in reduction of % biodiesel yield [20]. Therefore, 12:1 was the optimum methanol to oil molar ratio for sodium silicate catalyst which was 4 times higher than the required stoichiometric molar ratio and 24:1 was the optimum methanol to oil molar ratio which was higher 6 times higher than the required stoichiometric molar ratio.

Fig.11c, shows the effect of catalyst concentration on yield of biodiesel. To produce biodiesel from soybean triglyceride, the basic site of lithium silicate and sodium silicate generate a reactive nucleophile which was commonly known as methoxy-oxide from methanol which will react with electrophilic carbonyl carbon of triglyceride. This is the mechanism of transesterification reaction. Therefore, to enhance the biodiesel product, the amount of catalyst must be increased such that the active basic site will generally increase [36]. The result indicates that for sodium silicate catalyst, there was the increment of biodiesel from 45.3% to 96.4% as the catalyst content was increased from 1wt% to 2wt%; whereas 51.7% to 99.3% as the catalyst content was increased from

1wt% to 4wt% for lithium silicate catalyst. But, increasing the catalyst concentration beyond 3wt% for sodium silicate and beyond 4wt% for lithium silicate, did decrease the biodiesel yield because of limitation of mass transfer and high viscosity of reaction mixture [37].

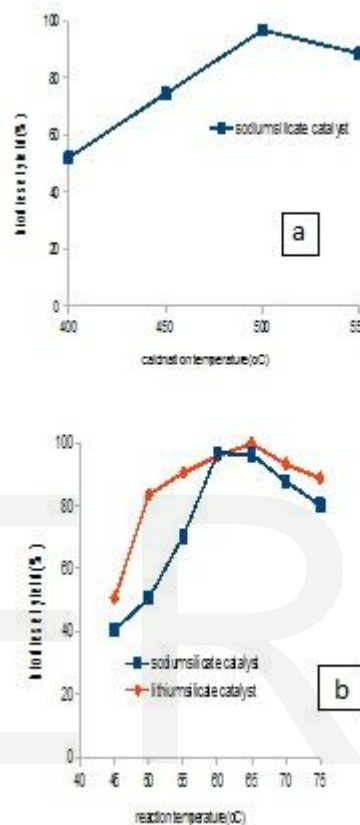


Fig. 10. (a) Effect of  $\text{Na}_2\text{SiO}_3$  calcination temperature on biodiesel yield (catalyst concentration: 3wt%, reaction temperature: 60 °C, methanol to oil ratio:12:1, reaction time:150min) and (b) Effect of reaction temperature on biodiesel yield (for  $\text{Na}_2\text{SiO}_3$ ; catalyst calcination=500°C, catalyst weight=3%, methanol:oil ratio=12:1, reaction time= 150min; for  $\text{Li}_2\text{SiO}_3$ ; catalyst weight= 4%, reaction time=180min, methanol:oil ratio= 24:1)

Using the optimized condition, the reusability of both RH based lithium silicate and sodium silicate catalyst were investigated (Fig.11d). After reusing of catalyst for 5<sup>th</sup> time, the yield of biodiesel was still about 83.7% and 75% respectively for sodium silicate and lithium silicate catalyst and the value falls to 45.8% for sodium silicate and 57.8% for lithium silicate catalyst after 7<sup>th</sup> run. Leaching of active species from catalytic site was the main possible reason for loss of catalytic activity [38][39]. Leaching of  $\text{Na}^+$  and  $\text{Li}^+$  to the reaction mixture was the main cause for the reduction in the yield of biodiesel after each cycle of run. Another possible reason for loss of activity was due to glycerol covering the surface of the catalyst.



## 5. CONFIRMATION OF BIODIESEL FUEL

### 5.1 Confirmation Using FTIR

General conclusion can be made about the transformation soybean triglyceride to biodiesel fuel methyl group around three possible peaks using FTIR technique (Fig.12). primarily due to O-CH<sub>3</sub> stretching of methyl group at 1164.90 cm<sup>-1</sup> with 0.5% transmittance for soybean oil, at 1170.00 cm<sup>-1</sup> with 15.5%T for RH derived sodium silicate catalyst based FAME product and at 1167.44cm<sup>-1</sup> with 43.5%T for RH derived lithium silicate catalyst based FAME. Due to the presence of methylene group of O-CH<sub>2</sub> at 1372.76 cm<sup>-1</sup> with 10.5%T for soybean oil, at 1366.69 cm<sup>-1</sup> with 38.8%T for RH derived sodium silicate catalyst based FAME product and at 1377.30 cm<sup>-1</sup> with 53.2%T for RH derived lithium silicate catalyst based FAME. Next, due to -CH<sub>3</sub> asymmetric bending vibration at 1458.73 cm<sup>-1</sup> with 0.25%T for soybean oil, at 1452.62 cm<sup>-1</sup> with 19.3%T for RH derived sodium silicate catalyst based FAME and at 1454.38 cm<sup>-1</sup> with 49.5%T for RH derived lithium silicate catalyst based FAME. In all above three region explanation, as the % transmittance of both biodiesel at those three point were greater than 18.5, this implies the biodiesel content of the product increases as those peaks increases correspondingly. The same result was reported by [40]. Therefore, the FTIR result confirms the transformation of oil triglyceride to biodiesel.

### 5.2 Confirmation Using H-NMR

The 1H NMR spectra of reactant soybean oil and RH-derived sodium silicate and lithium silicate catalyst based FAME, were shown in Fig.13. The presence of peak at 3.66ppm (the peak which corresponds to the presence of methyl ester proton of biodiesel) was visible in Fig.13b & c; which marks the representative variance in the 1H NMR spectra of mother soybean compound and its derivatives biodiesel. The non-appearance of doublet of doublet peak at 4.2ppm is another remarkable story in the 1H NMR of fatty acid methyl ester produced by RH-derived sodium silicate and lithium silicate catalysts. It is clearly observed that, for both fatty acid methyl ester 1H NMR, there is no signal in between 4.0ppm and 5.2ppm which confirms the high conversion yield of soybean oil triglyceride in to biodiesel [41]. The glyceridic protons of the triglyceride, diglyceride and mono glyceride were appeared at the doublet of doublet peak in the range of 4.0 – 4.3 ppm; which in turn confirm the progress of transesterification reaction. This value is diminished in the biodiesel spectrum and this signifies the formation of fatty acid methyl ester that is observed at the peak of 3.66 ppm [41, [42].

### 5.3 Confirmation using GC-MS

The result of fatty acid methyl ester obtained after transesterification of soybean oil using RH based sodium silicate and RH based lithium silicate alkali catalyst were as shown in the Fig. 14.

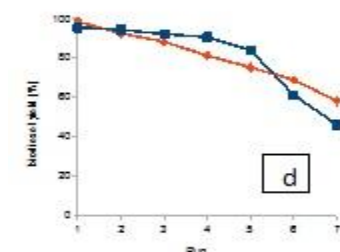
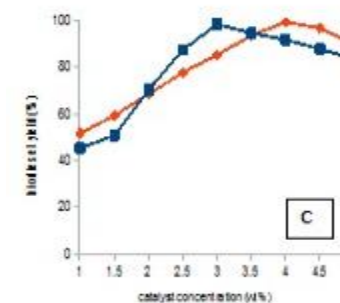
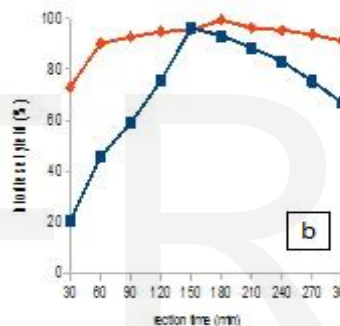
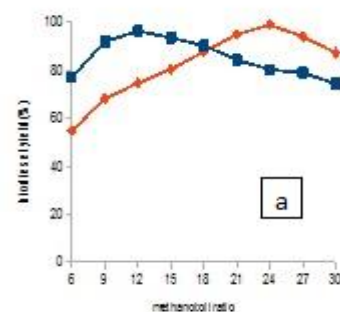




Fig. 11. (  Sodium Silicate,  Lithium Silicate catalyst) Effect of methanol to oil molar ratio (a), reaction time (b), catalyst concentration (c) and reusability of the catalyst (d)

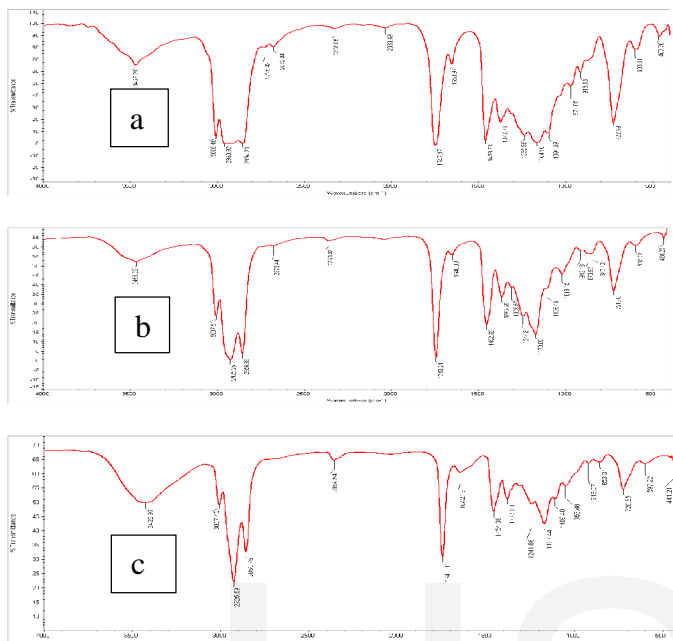


Fig. 12. FTIR spectra (Wavenumber,  $\text{cm}^{-1}$  Vs. Transmittance, %) of soybean oil (a), rice husk derived sodium silicate catalyst based FAME (b), rice husk derived lithium silicate catalyst based FAME(c)

Retention time(min)		Area (0.1 $\mu\text{m}$ Vx sec)		Component name	Solution conc.(ppm)	
A	B	A	B		A	B
4.667	3.750	24232	3457	C14:0	0.069	0.006
7.250	7.000	70562	122202	C16:0	0.202	0.212
8.750	7.667	356792	70008	C18:0	1.023	0.121
12.500	8.750	53031	825225	C18:1	0.152	1.429
13.417	11.000	379752	27302	C18:2	1.089	0.047
15.083	12.500	823446	112584	C18:3	2.360	0.195
16.583	13.417	20819	697412	C20:0	0.060	1.208
17.167	15.083	102014	1608508	C20:1	0.292	2.785
19.083	16.583	5908	17863	C20:2	0.017	0.031
24.750	17.167	55594	182308	C20:3	0.159	0.316
25.917	20.333	26602	24614	C21:0	0.076	0.043
30.583	22.833	115960	41958	C22:1	0.332	0.073

TABLE 2.

FATTY ACID PROFILE OF SOYBEAN OIL METHYL ESTER CONVERTED BY CATALYST A) RH- $\text{Na}_2\text{SiO}_3$ , B) RH- $\text{Li}_2\text{SiO}_3$

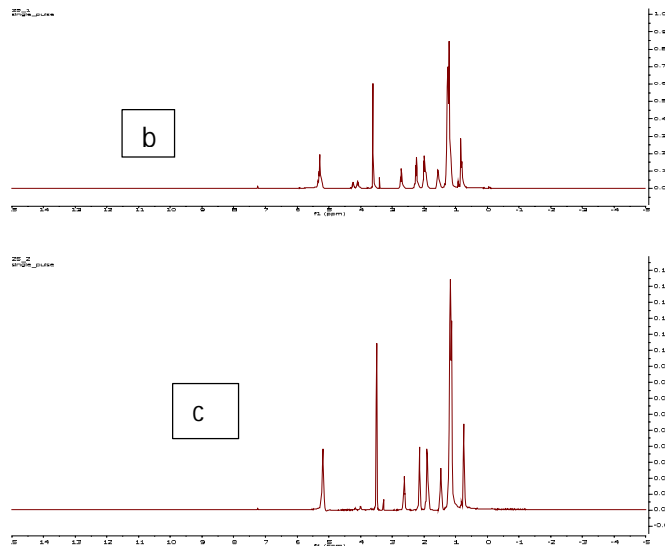
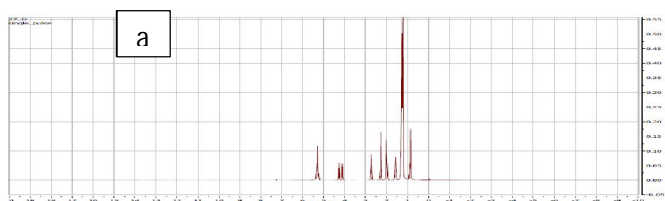


Fig.13. H-NMR for soybean oil (a), FAME obtained by RH- $\text{Na}_2\text{SiO}_3$  catalyst (b) and FAME obtained by RH- $\text{Li}_2\text{SiO}_3$  catalyst (c)

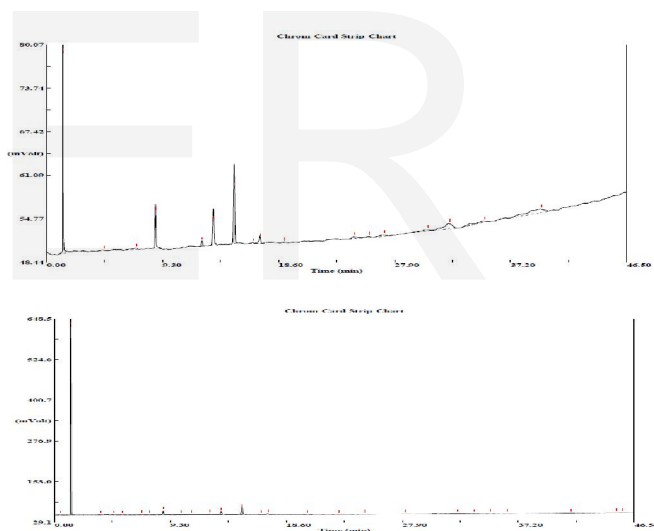


Fig. 14. GC-MS spectra for FAME obtained by RH- $\text{Na}_2\text{SiO}_3$  catalyst (a) and FAME obtained by RH- $\text{Li}_2\text{SiO}_3$  catalyst (b)

From Table 2, the same fatty acid profile were detected by both catalyst at different retention time, with different peak area and with different solution concentration. Using RH- $\text{Na}_2\text{SiO}_3$  catalyst, methyl linolenate (C18:3) was detected at 15.083min with relatively highest concentration of 2.360ppm and using RH- $\text{Li}_2\text{SiO}_3$  catalyst, methyl eicosonate (C20:1) was

detected at 15.083min with relatively highest concentration of 2.785ppm.

## 6. PHYSIOCHEMICAL PROPERTIES OF BIODIESEL FUEL

As shown from Table 3, the physiochemical properties of biodiesel produced by both catalysts were confirming to all standard conditions.

## 7. CONCLUSION

This study developed synthesis of  $\text{Li}_2\text{SiO}_3$  and  $\text{Na}_2\text{SiO}_3$  by solid-state reaction from rice husk ash as catalysts for the application of biodiesel production directly without further catalyst synthesis process. The experimental result showed that  $\text{Li}_2\text{SiO}_3$  and  $\text{Na}_2\text{SiO}_3$  catalysts demonstrated excellent catalytic activity because of their high basic strength and their stability in transesterification reaction. At optimum condition of 500°C catalyst calcination, 3wt% catalyst concentration, 60°C reaction temperature, 150min reaction time and 12:1 methanol to oil molar ratio; the biodiesel yield of 96.7% was obtained for rice husk derived sodium silicate catalyst. Whereas for rice husk derived lithium silicate catalyst, the biodiesel yield of 99.4% was obtained at optimum condition of 4wt% catalyst concentration, reaction temperature of 65°C, reaction time of 180min and methanol to oil ratio of 24:1. The biodiesel fuel synthesized by catalysts was characterized by FTIR, H-NMR and GC-MS and the result confirms the transformation of oil triglyceride to methyl group of biodiesel fuel.

## ACKNOWLEDGEMENT

Authors wish to thank Dean, School of Meechanical Chemical and Materials Engineering, Adama Science and Technology University, Adama, Ethiopia and Institute Instrumentation Centre (IIC), Indian Institute of Technology Roorkee (IITR), Utrakhand, India for the facilities extended for completing this study.

## REFERENCE

- [1] Memon SA, Shaikh MA, Akbar H. Utilization of Rice Husk Ash as Viscosity Modifying Agent in Self Compacting Concrete, *Constr Build Mater*, vol. 25, pp. 1044-1048, 2011.
- [2] Subbukrishna DN, Suresh KC, Paul PJ, Dasappa S, Rajan NKS, Precipitated Silica from Rice Husk Ash by IPSIT Process. 15th European Biomass Conference and Exhibition, Berlin, Germany, 7-11 May 2007.
- [3] Armesto L, Bahillo A, Veijonen K, Cabanillas A, Otero J. Combustion Behavior of Rice Husk in a Bubbling Fluidized Bed, *Biomass Bioenergy*, vol. 23, pp. 171-179, 2002.
- [4] Mane VS, Deo Mall I, Chandra Srivastava V, Kinetic and Equilibrium Isotherm Studies for the Adsorptive Removal of Brilliant Green Dye from Aqueous Solution by Rice Husk Ash, *J Environ Manage*, vol. 84, pp. 390-400, 2007.
- [5] Fuad MYA, Ismail Z, Ishak ZaM, Omar AKM, Application of Rice Husk Ash as Fillers in Polypropylene: Effect of Titanate, Zirconate and Silane Coupling Agents, *Eur Polym J*, vol. 31, pp. 885-893, 1995.
- [6] Zerbino R, Giaccio G, Isaia GC. Concrete Incorporating Rice-Husk Ash without Processing, *Constr Build Mater*, vol. 25, pp. 371-8, 2011.

Fuel properties, unit	Standard method	Limits of bio diesel	Soybean Oil	Soybean biodiesel fuels	
				RH- $\text{Na}_2\text{SiO}_3$	RH- $\text{Li}_2\text{SiO}_3$
Density, $\text{kg m}^{-3}$	BIS	860-900	912	880	880.1
Kinematic viscosity 30 °C, $\text{mm}^2 \text{s}^{-1}$	ASTM D6751	1.9-6.0	35	4.181	4.170
Saponifi-cation value, mg KOH $\text{g}^{-1}$ oil	AOCS	-	189.44	173.0	170.8
Acid value, mg KOH $\text{g}^{-1}$ oil	D664	$\leq 0.8$	0.583	0.3020	0.3000
Ash content, %	D975	$\leq 0.01$	0.024	0.0090	0.0060
Cloud point, °C	-	-3 to 10	-9	1	-2
Pour point, °C	-	-15 to 10	-12	-4.5	-6
Fire point, °C	-	-	314	216	213
Flash point, °C	D93	$\geq 130$	280	202	199.4
Heating value, $\text{MJ kg}^{-1}$	D2015	39-43.3	38.95	39.48	39.43

TABLE 3.  
PHYSIOCHEMICAL PROPERTIES OF SOYBEAN OIL AND SOYBEAN BIODIESEL FUEL PRODUCED BY BOTH CATALYSTS.

- [7] Krishnarao RV, Subrahmanyam J, Jagadish Kumar T. Studies on the Formation of Black Particles in Rice Husk Silica Ash, *J Eur Ceram Soc*, vol. 21, pp. 99-104, 2001.
- [8] Prasetyoko D, Ramli Z, Endud S, Hamdan H, Sulikowski B, Conversion of Rice Husk Ash to Zeolite Beta, *Waste Manage*, vol. 26, pp. 1173-1179, 2006.
- [9] Vieira MGA, Neto AFDA, Silva MGCD, Carneiro CN, Filho AaM. Influence of the System on Adsorption of Pb(II) and Cu(II) by Rice Husks Ash: Kinetic Study. *Chem Eng Trans*, vol. 24, pp. 1213-1218, 2011.
- [10] Ali IO., Hassan AM, Shaaban SM, Soliman KS, Synthesis and Characterization of ZSM-5 Zeolite from Rice Husk Ash and their Adsorption of Pb<sup>+</sup> onto Unmodified and Surfactant-Modified Zeolite, *Separ Purif Technol*, vol. 83, pp. 38-44, 2011.
- [11] Chowdhury S, Mishra R, Saha P, Kushwaha P. Adsorption Thermodynamics Kinetics and Isotheric Heat of Adsorption of Malachite Green onto Chemically Modified Rice Husk. *Desalination*, vol. 265, pp. 159-168, 2011.
- [12] Zain MFM, Islam MN, Mahmud F, Jamil M, Production of Rice husk Ash for Use in Concrete as a Supplementary Cementitious Material, *Construction and Building Materials*, vol. 25, no. 2, pp. 798-805, 2011.
- [13] Magale KDR, Andre LC, Daiane BB, Tiele Mi, Luceilia AR, Gaspar HK, Ayrton FM, Silica from Rice Husk Ash an Additive for Rice Plant, *Journal of Agronomy*, vol. 10, no. 3, pp. 99-104, 2011.
- [14] Geetha D, Ananthi A, Ramesh PS, Preparation and Characterization of Silica Material from Rice Husk Ash-An Environmentally Viable Method, *Research and Reviews: Journal of Pure and Applied Physics*, 2016.



- [15] An D, Guo Y, Zou B, Zhu Y, Wang Z, A Study on the Consecutive Preparation of Silica Powders and Active Carbon from Rice Husk Ash, *Biomass and Bioenergy*, vol. 35, no. 3, pp. 1227-1234, 2011.
- [16] Arantes RS, Lima RMF. Influence of Sodium Silicate Modulus on Iron Ore Flotation with Sodium Oleate, *Int J Miner Process*, vol. 125, pp. 157-160, 2013.
- [17] Yun-yu Z, Xiao-xuan L, Zheng-xing C, Rapid Synthesis of Well-Ordered Mesoporous Silica from Sodium Silicate, *Powder Technol*, vol. 226, pp. 239-245, 2012.
- [18] Selvam T, Bandarapu B, Mabande GTP, Toufar H, Schwieger H, Hydrothermal Transformation of a Layered Sodium Silicate, Kanemite, into Zeolite Beta (BEAT), *Microporous Mesoporous Mater*, vol. 64, pp. 41-50, 2003.
- [19] He F, Wang X, Wu D, Phase-change Characteristics and Thermal Performance of Form-Stable n-alkanes/Silica Composite Phase Change Materials Fabricated by Sodium Silicate Precursor. *Renew Energy*, vol.74, 689-698, 2015.
- [20] Guo F, Peng ZG, Dai JY, Xiu ZL, Calcined Sodium Silicate as Solid Base Catalyst for Biodiesel Production, *Fuel Process Technol*, vol 91, pp. 322-328, 2010.
- [21] Long YD, Guo F, Fang Z, Tian XF, Jiang LQ, Zhang F, Production of Biodiesel and Lactic Acid from Rapeseed Oil Using Sodium Silicate as Catalyst, *Bioresour Technol*, vol. 102, no. 13, pp. 6884-6886, 2011.
- [22] Guo F, Wei NN, Xiu ZL, Fang Z, Transesterification Mechanism of Soybean Oil to Biodiesel Catalysed by Calcined Sodium Silicate, *Fuel*, vol. 93, pp. 468-472, 2012.
- [23] Kongmanklang C, Rangsiwatananon K, Hydrothermal Synthesis of High Crystalline Silicalite from Rice Husk Ash, *J Spectrosc*, 2015.
- [24] Leung DYC, Guo Y, Transesterification of Neat and Used Frying Oil: Optimization for Biodiesel Production, *Fuel Processing Technology*, vol. 87, no. 10, pp. 883-890, 2006.
- [25] Umeda J, Kondon K, Process Optimization to Prepare High Purity Amorphous Silica from Rice Husks via Citric Acid Leaching Treatment, *Transactions of JWRI*, vol. 37, pp 13-17, 2008.
- [26] Nayak JP and Bera J. Preparation of an Efficient Humidity Indicating Silica Gel from Rice Husk Ash. *Bull. Mater. Sci*, vol. 34, pp. 1683-1687, 2011.
- [27] Kalapathy U, Proctor A, Shultz J, An Improved Method for Production of Silica from Rice Hull Ash. *Bioresource Technology*, vol. 85, no. 3, pp. 285-289, 2002.
- [28] Farook Adam, Jeyashelly Andas, Ismail Ab. Rahman, The Synthesis and Characterization of Cobalt-Rice Husk Silica Nanoparticles, *The Open Colloid Science Journal*, vol. 4, pp. 12-18, 2011.
- [29] Martin-Luengo MA, Yates M, Diaz M, Renewable Fine Chemicals from Rice and Citric Subproducts, Ecomaterials, *Applied Catalysis B: Environmental*, vol. 106, pp. 488-493, 2011.
- [30] Srivastava, VC, Mall, ID, Mishra, IM, Characterization of Mesoporous Rice Husk Ash (RHA) and Adsorption Kinetics of Metal Ions from Aqueous Solution onto RHA. *J. Hazard. Mater.*, vol. 134, pp. 257-267, 2006.
- [31] Tarley, C. R. T., Ferreira, S. L. C. and Arruda, M. A. Z. Use of Modified Rice Husks as a Natural Solid Adsorbent of Trace Metals: Characterization and Development of on-line Pre Concentration System for Cadmium and Lead determination by FAAS. *Microchem. J.*, vol. 77, pp. 163-175, 2004.
- [32] Mohamed Mahmoud, M, Folz, DC, Suchicital, TAC, Clark, DE, Crystallization of Lithium Di-silicate Glass using Microwave Processing. *J. Amer. Chem. Soc.* Vol. 95, pp. 579-585, 2012.
- [33] Efimov, AM, Pogareva VG, Parfinskii VN, Okatov MA, Tolmachev VA, Infrared Reflection Spectra, Optical Constants and Band Parameters of Binary Silicate and Borate Glasses Obtained from Water Free Polished Sample Surfaces, *Glass Technology*. vol. 46, no. 1, pp. 20-27, 2005.
- [34] Ortiz LJ, Contreras Garcı́a ME, Go´mez Ya´n´ez C, Pfeiffer H. Surfactant-Assisted Hydrothermal Crystallization of Nanostructured Lithium Metasilicate (Li<sub>2</sub>SiO<sub>3</sub>) Hollow Spheres: (I) Synthesis, Structural and Microstructural Characterization, *J Solid State Chem*, vol. 184, pp 1304-1311, 2011.
- [35] Chen GY, Shan R, Shi JF, Yan BB. Trans-esterification of Palm Oil to Biodiesel using Rice Husk Ash-Based Catalysts, *Fuel Process Technol*, vol. 133, pp. 8-13, 2015.
- [36] Roschat W, Kacha M, Yoosuk B, Sudyoadsuk T, Promarak V. Biodiesel Production Based on Heterogeneous Process Catalyzed by Solid Waste Coral Fragment, *Fuel*, vol. 98, pp. 194-202, 2012.
- [37] Dai YM, Wu JS, Chen CC, Chen KT. Evaluating the Optimum Operating Parameters on Transesterification Reaction for Biodiesel Production Over a LiAlO<sub>2</sub> Catalyst, *Chem Eng J.*, vol. 280, pp. 370-376, 2015.
- [38] Shan R, Chen G, Yan B, Shi J, Liu C, Porous CaO-Based Catalyst Derived from PSS Induced Mineralization for Biodiesel Production Enhancement, *Energy Convers Manage*, vol. 106, pp. 405-413, 2015.
- [39] Syazwani ON, Rashid U, Yap YHT, Low-Cost Solid Catalyst Derived from Waste Cyrtopleura Costata (Angel Wing Shell) for Biodiesel Production using Microalgae Oil, *Energy Convers Manage*, vol. 101, pp. 749-756, 2015.
- [40] Tao Yuan, Emmanuel Akochi-Koble, Dave Pinchuk and Frederik R. van de Voort, *International Journal of Renewable Energy & Biofuels*, 2014, DOI: 10.5171/2014.178474
- [41] M. Morgenstern, J. Cline, S. Meyer, S. Cataldo, Determination of the Kinetics of Biodiesel Production using Proton Nuclear Magnetic Resonance Spectroscopy (1H NMR), *Energy Fuels*, vol. 20, pp. 1350-1353, 2006.
- [42] Monteiro, MR, Ambroziu, ARP, Liao, LM, Ferreira AG, Determination of Biodiesel Blend Levels in Different Diesel Samples by 1H NMR, *Fuel*, vol. 88, pp. 691-696, 2009.